

Ultrafast optical nonlinearity in quasi-one-dimensional Mott-insulator Sr_2CuO_3

T. Ogasawara¹, M. Ashida², N. Motoyama¹, H. Eisaki¹, S. Uchida¹, Y. Tokura¹, H. Ghosh³, A. Shukla^{2,3}, S. Mazumdar³, M. Kuwata-Gonokami^{1,2*}

¹*Department of Applied Physics, the University of Tokyo,
7-3-1, Hongo, Bunkyo-ku, Tokyo, 113-8656, Japan*

²*Cooperative Excitation Project, Japan Science and Technology Corporation (JST),
3-2-1 Sakato, Takatsu-ku, Kanagawa 213-0012, Japan*

³*Department of Physics and The Optical Sciences Center,
University of Arizona, Tuscon, AZ85721, USA*

(October 23, 2018)

Abstract

We report strong instantaneous photoinduced absorption in the quasi-one-dimensional Mott insulator Sr_2CuO_3 in the IR spectral region. The observed photoinduced absorption is to an even-parity two-photon state that occurs immediately above the absorption edge. Theoretical calculation based on a two-band extended Hubbard model explains the experimental features and indicates that the strong two-photon absorption is due to a very large dipole-coupling between nearly degenerate one- and two-photon states. Room temperature picosecond recovery of the optical transparency suggests the strong potential of Sr_2CuO_3 for all-optical switching.

Nonlinear optical materials with large nonlinear coefficient, fast response-time, low loss and operability at room-temperature will be indispensable for next generation high speed network systems in which clock recovery and buffering at terabit/second rate will be performed by all-optical switches [1]. These devices should operate in the transparent region below the fundamental band edge, where optical nonlinearity is mainly associated with two-photon absorption (TPA). Real carrier excitation, inevitable due to TPA, is considered as the major limiting factor here. Although terabit/second all-optical switches have been already demonstrated with conventional inorganic band semiconductors [2], considerable effort is necessary to overcome the difficulty associated with long carrier lifetime. Large optical nonlinearity and sub-picosecond response times are observed in organic π -conjugated polymers [3,4], but further improvements in sample quality and morphology would be required for actual applications. Parallel development of novel nonlinear optical inorganic materials that on the one hand possess the large nonlinearity and ultrafast recovery times of the organics, and the intrinsic robustness and superior thermal conductivity of inorganics on the other, is highly desirable. To date, no such inorganic semiconductor is known. We report in the present Letter the observation of large ultrafast optical nonlinearity in a novel strongly correlated inorganic semiconductor that is intrinsically different from conventional inorganic band semiconductors. The specific material we have studied is Sr_2CuO_3 .

Sr_2CuO_3 is a quasi-1D Cu-O linear chain compound, whose structure is shown in Fig. 1(a). The material is a prototypical strongly correlated charge-transfer insulator within the Zaanen-Sawatzky-Allen scheme [5]. Optical absorption in Sr_2CuO_3 involves charge-transfer (CT) excitation of a Cu-hole to an O-site, with an absorption band-edge at ~ 1.6 eV and the band maximum at 2 eV (Fig. 1(b)). In addition to the high energy charge excitations, there exist low energy spin excitations in Sr_2CuO_3 , which correspond to those of a nearly ideal 1D Heisenberg chain with intrachain exchange integral $J \sim 2000 - 3000$ K [6,7]. The interchain coupling in this system is rather weak, as is evidenced by the occurrence of 3D long-range antiferromagnetic coupling only below $T_N = 5$ K [8].

We present here the results of time-resolved femtosecond pump-probe measurements on

a single crystal of Sr_2CuO_3 , grown by the traveling-solvent floating-zone method [7]. A thin flake with a thickness of $L \sim 50 \mu\text{m}$ was cleaved out with the bc -plane for transmission measurement. Optical pulses are provided by a system based on amplified mode-locked Ti:sapphire laser and optical parametric generator supplemented with sum and difference frequency generation. This system generates pulses with the photon energy centered at 0.2 – 2.0 eV and with temporal width ~ 200 fs. In our experiment, we measure the differential transmission $\Delta T/T$ (where T is the transmission in the absence of the pump beam), as a function of the delay time of the probe with respect to the pump.

Fig. 1(c) shows the temporal evolution of $\Delta T/T$ measured at 10 K for different pump (ω_{pump}) and probe (ω_{probe}) photon energies. The intensity of the pump pulse is $\sim 2 \text{ GW}/\text{cm}^2$. The intensity of the probe pulse is one to two orders of magnitude smaller. One can observe from Fig. 1(c) that the differential transmission consists of two components. The first component manifests itself as a sharp peak-like structure with temporal width of about 200 fs, which is given by the overlapping of pump and probe pulses. This component, which is pronounced when the pump photon energy is tuned below the absorption edge of ~ 1.6 eV, is due to coherent interaction between the pump and probe pulses. At $\omega_{\text{pump}} = 3.1$ eV, which is far above the absorption edge, this coherent interaction is suppressed by the strong linear absorption, and correspondingly, the peak-like structure in the pump-induced transmission vanishes. At $\omega_{\text{pump}} = 1.55$ eV, the strong group velocity dispersion near the absorption edge gives rise to the increase in the temporal width of the peak-like structure up to approximately 1 ps.

The second component of the transmission change manifests itself as an exponentially decaying tail with characteristic time of about 2 ps. One can observe from Fig. 1(c) that magnitude of this component decreases with decreasing of the pump photon energy and, correspondingly, with the pump absorption coefficient (see Fig. 1(b)). These experimental findings indicate that this relatively long-lived component of the transmission change can be associated with real excitation of the CT exciton, whose decay time is of similar magnitude.

These features in the temporal behavior of the pump-induced transmission remain at

room temperature. We find that the magnitude of the effect is proportional to the pump intensity up to $\sim 5 \text{ GW/cm}^2$, indicating the pump-induced transmission change to be a third order optical process.

We describe $\Delta T/T$ in terms of the pump-induced change in the absorption coefficient $\Delta\alpha = -\ln(1 + \Delta T/T)/L$, where L is the crystal length, which consists of the instantaneous (peak) and exponentially decaying (tail) components, respectively: $\Delta\alpha = \Delta\alpha_{\text{peak}} + \Delta\alpha_{\text{tail}}$. Fig. 2(a) shows the spectrum of TPA coefficient $\beta = \Delta\alpha_{\text{peak}}/I_{\text{pump}}$ as a function of ω_{probe} for pump photon energies of 0.7 eV, 1.1 eV and 1.55 eV. One can observe from Fig. 2(a) that the smaller the ω_{pump} , the larger is the probe photon energy ω_{probe} at which the maximum of the pump-induced coherent absorption is obtained. Moreover, it is seen that β is maximum at $\omega_{\text{probe}} \approx 2.1 \text{ eV} - \omega_{\text{pump}}$ at all pump photon energies. This strongly suggests that the peak structure in Fig. 1 (c) is due to a two-photon allowed (one-photon forbidden) state at $\sim 2.1 \text{ eV}$. Alternative mechanisms, which may be responsible for the observed instantaneous photoinduced absorption change, can in principle involve fifth- and higher order effects associated with real carriers excitation due to two-photon absorption of the pump or with the electron-hole plasma created by the intense pump pulse [9]. However, the observed linear dependence of $\Delta\alpha_{\text{peak}}$ on the pump intensity suggests that the instantaneous photoinduced absorption is essentially of the third-order in the light field. This observation along with the strong dependence of the pump-induced transmission spectra on ω_{pump} precludes mechanisms of optical nonlinearity other than TPA.

To clarify this further we plot β in Fig. 2(b) as a function of $\omega_{\text{pump}} + \omega_{\text{probe}}$. One can readily observe that maximum of the pump-induced coherent absorption takes place at $\omega_{\text{pump}} + \omega_{\text{probe}} = 2.1 \text{ eV}$ for all pump photon energies. The dashed line on Fig. 2(b) represents the linear absorption spectrum indicating that one- and two-photon allowed bands nearly overlap.

In order to clarify the origin of the observed TPA band in Fig. 2(b) we consider the Cu-O chain within the two-band extended Hubbard model [10],

$$H = \sum_i U_i n_{i\uparrow} n_{i\downarrow} + V \sum_i n_i n_{i+1} + \sum_{i,\sigma} (-1)^i \epsilon n_i - t \sum_{i,\sigma} (c_{i\sigma}^\dagger c_{i+1\sigma} + c_{i+1\sigma}^\dagger c_{i\sigma}) \quad (1)$$

where $c_{i\sigma}^\dagger$ creates a hole with spin σ on site i , $n_{i\sigma} = c_{i\sigma}^\dagger c_{i\sigma}$, and $n_i = \sum_\sigma n_{i\sigma}$. The parameter t is the transfer integral between Cu and O sites, $2\epsilon = \epsilon_O - \epsilon_{Cu}$, where ϵ_O and ϵ_{Cu} are the site energies of the O and Cu sites, U_i is the on-site Coulomb repulsion between two holes on Cu and O sites ($U_{Cu} \neq U_O$) and V is the Coulomb repulsion between holes occupying neighboring Cu and O sites. For large U_i and realistic $\epsilon > 0$, the holes occupy predominantly the Cu sites in the ground state, which can thus be represented by the hole occupancy scheme ..101010...., where 1(0) represents an occupied(unoccupied) site. From the nature of the current operator $\hat{j} = -it \sum_{i,\sigma} (c_{i\sigma}^\dagger c_{i+1\sigma} - c_{i+1\sigma}^\dagger c_{i\sigma})$, the one-photon optical state has the form (...10100110...) - (...10110010...), i.e., the odd parity linear combination of the two configurations that are reached by one application of the current operator on the ground state. The even parity “plus” linear combination of the same two configurations is a two-photon state, which for strong correlations is nearly degenerate with the one-photon state. This near degeneracy is expected to lead to very large transition dipole coupling between the one- and two-photon states.

To confirm the above conjecture we have performed exact numerical calculations for finite periodic rings of 12 sites (6 Cu and 6 O) within Eq.1, for parameters $|t| = 1 - 1.4$ eV, $U_{Cu} = 8 - 10$ eV, $U_O = 4 - 6$ eV, $V = 0 - 2$ eV, and $\epsilon = 1 - 2$ eV. Because of the large Hubbard U the relevant wavefunctions are strongly localized, and even the 12-site periodic ring can give semi-quantitative results. In all cases, the transition dipole coupling between the one- and the two-photon states is one to two orders of magnitude larger than that between the ground state and the one-photon state. The third order nonlinear optical coefficient, $\chi^{(3)}(-\omega; \omega, \omega, -\omega)$, whose imaginary component gives the TPA, is now calculated from the energies and transition dipole couplings [11]. In Fig. 3 we have shown the calculated absorption and TPA spectra in arbitrary units, for one set of parameters for our finite system. The inset shows the energies of the one- and two-photon states and the transition dipole couplings that are used in the calculation.

At the maximum of the TPA band, the magnitude of the experimental TPA coefficient β is ~ 150 cm/GW (Fig. 2(b)), which corresponds to $\text{Im}\chi^{(3)} \sim 10^{-9}$ esu. This value is larger than that predicted from the gap-dependent scaling law derived for conventional semiconductors [12] by one order of magnitude, and is comparable to that of conventional 1D-structured materials. The scaling law [12] is inapplicable to Mott-insulators, in which the origin of the optical nonlinearity is the very large dipole coupling between nearly degenerate excited states of opposite parities. The mechanism of optical nonlinearity here is related to that in the π -conjugated polymers, which are described within the *one*-band extended Hubbard model and in which also there occurs very large dipole coupling between the optical state and a two-photon state slightly higher in energy [13]. Not surprisingly, the magnitude of $\chi^{(3)}$ in Sr_2CuO_3 is therefore comparable to some of the best organic materials [14,15]. The intensity dependent refractive index n_2 , obtained by a Kramers-Kronig transformation of the TPA data, is $\sim 10^{-7} - 10^{-6}$ cm²/MW, also comparable to the organics [14].

In addition to the large magnitude, the excitonic nonlinearity in Sr_2CuO_3 is featured by picosecond response, whose characteristic time is given by the decay constant of the tail-like component in Fig. 1(c). Such an ultrashort response indicates the existence of a fast non-radiative relaxation channel. Although detailed discussion of relaxation mechanisms of the optical excitation in Sr_2CuO_3 is beyond the scope of this paper, we suggest that the ultrafast ground state recovery is related to the occurrence of spin excitations below the optical gap [16,17]. The low energy excitations of these system are the gapless spin excitations (spinons) of the uniform one-dimensional antiferromagnetic Heisenberg chain. These spin excitations are optically silent, and have an overall bandwidth of ~ 1 eV [6,7]. It is then conceivable that following the relaxation of the CT exciton to the highest energy spin excited states there occur further fast intra-spinon-band relaxation through the emission of multiple phonons and spinons. Because of the absence of such midgap states in the conventional semiconductors similar non-radiative processes would be absent there.

The room temperature ultrafast ground state recovery implies a high potential of Sr_2CuO_3 in the ultrafast optoelectronics and, specifically, in all-optical switching devices. In

order to estimate this potential in terms of the maximum available repetition rate, we have performed a double-pulse experiment at room-temperature. Fig. 4 shows the $\Delta T/T$ induced by two pump pulses with wavelength of 1400 nm. The transmission change was measured at 1200 nm, which is around the optical fiber communication wavelength. The second pump pulse, applied 2 ps after the first, induces nearly the same transmission change as the first. However, comparing with the single-pulse response (not shown), the transmission change in tail part is accumulated from pulse to pulse, leading to the limitation on the repetition rate. If $\Delta\alpha_{\text{tail}}$ and $\Delta\alpha_{\text{peak}}$ are the tail and peak components of photoinduced absorption and f is the pulse repetition rate, the tail component of the induced absorption in the steady-state regime is $\delta\alpha_{\text{tail}} = \Delta\alpha_{\text{tail}}/[1 - \exp(-1/\tau f)]$. Therefore, the maximum available repetition rate can be estimated from a natural criterion of the operability of the system, $\delta\alpha_{\text{tail}} = \Delta\alpha_{\text{peak}}$, which gives $f_{\text{max}} = (\Delta\alpha_{\text{peak}}/\Delta\alpha_{\text{tail}})\tau^{-1}$. From Fig. 4, we obtain $f_{\text{max}} \approx 10^{13}\text{s}^{-1}$ for our sample, i.e., it can be used as a nonlinear optical medium with operability of several terabits per second.

In summary, we find that Sr_2CuO_3 exhibits strong nonlinearity and picosecond recovery of optical transparency. Theoretical calculations indicates that the nonlinearity of the quasi-1D cuprates is due to a very large transitional dipole moment between nearly degenerate one- and two-photon states. Our findings suggest a strong potential of these materials for high bit-rate all-optical switching and, therefore, introduce a new means of achieving ultrafast optoelectronics with strongly correlated electron systems. We believe that with innovative material processing there is considerable scope for future enhancement of the figure of merit of these materials for optoelectronic applications.

This work was supported by a grant-in-aid for COE Research from the Ministry of Education, Science, Sports, and Culture of Japan, and the U.S. NSF-ECS.

REFERENCES

- * Author to whom correspondence should be addressed. Electronic address: gonokami@ap.t.u-tokyo.ac.jp
- [1] G. I. Stegeman, and A. Miller, Physics of all-optical switching devices, in *Photonics in Switching*, J. E. Midwinter, ed. (Academic, San Diego, CA, 1993), Vol.1, Ch. 5.
- [2] Shigeru Nakamura, Yoshiyasu Ueno, and Kazuhiko Tajima, IEEE Photonics Technology Letters **10**, 1575 (1998).
- [3] *Nonlinear Optical Properties of Organic Molecules and Crystals*, edited by D.S. Chemla and J. Zyss, (Academic, Orlando, 1987).
- [4] *Nonlinear Optical Effects in Organic Polymers*, edited by J. Messier et al., (Kluwer, Boston, 1988).
- [5] J. Zaanen, G. A. Sawatzky, and J. W. Allen, Phys. Rev. Lett. **55**, 418 (1985).
- [6] H. Suzuura, H. Yasuhara, A. Furusaki, N. Nagaosa, and Y. Tokura, Phys. Rev. Lett. **76**, 2579 (1996).
- [7] N. Motoyama, H. Eisaki, and S. Uchida, Phys. Rev. Lett. **76**, 3212 (1996).
- [8] A. Keren, *et al.*, Phys. Rev. B **48**, 12926 (1993).
- [9] Since the exciton in the strongly correlated charge-transfer insulator has a very large binding energy, exciton ionization can not occur at our pump intensities. This is in strong contrast with conventional semiconductors, in which the exciton motte transition takes place at a moderate excitations.
- [10] M. Imada, A. Fujimori, and Y. Tokura, Rev. Mod. Phys. **70**, 1039 (1998).
- [11] R. W. Boyd, *Nonlinear Optics*, Academic Press (London, 1992).
- [12] E. W. Van Stryland, M. A. Woodall, H. Vanherzeele, and M. J. Soileau, Opt. Lett. **10**,

490 (1985).

[13] M. Chandross, Y. Shimoi, and S. Mazumdar, Phys. Rev. B **59**, 4822 (1999).

[14] B. Lawrence, *et al.*, Phys. Rev. Lett. **73**, 597 (1994).

[15] A. Mathy *et al.*, Phys. Rev. B **53**, 4367 (1996).

[16] K. Matsuda, *et al.*, Phys. Rev. B **50**, 4097 (1994).

[17] K. Matsuda, *et al.*, Physica C **280**, 84 (1997).

FIGURES

FIG. 1. (a) Crystal structure of Sr_2CuO_3 . (b) Absorption spectrum of Sr_2CuO_3 , obtained by Kramers-Kronig transformation of reflectivity. The solid triangles (i) – (iv) indicate the pump photon energies in (c). (c) Temporal evolution of $\Delta T/T$, measured at various pump and probe photon energies at ~ 10 K. The temporal evolution consists of two components: the hatched peak-like structure corresponds to coherent interaction of two pulses, and the exponential tail corresponds to incoherent charge-transfer excitation induced absorption. The relaxation times τ are the best fits to the exponential tails.

FIG. 2. Spectra of photoinduced absorption efficiency $\beta(\omega_{\text{probe}}; \omega_{\text{pump}})$, for pump energies of (i) 0.7 eV, (ii) 1.1 eV, and (iii) 1.55 eV (~ 10 K). The solid lines are guides to the eye. (b) β vs. sum of the pump and probe photon energy $\omega_{\text{pump}} + \omega_{\text{probe}}$, for four different pump energies (~ 10 K). The dotted line is the linear absorption $\alpha(\omega)$, which is plotted with the same energy scale as $\omega_{\text{pump}} + \omega_{\text{probe}}$ for comparison.

FIG. 3. The calculated linear absorption and TPA spectra of our finite periodic ring in arbitrary units (the TPA spectrum is plotted against 2ω), for $U_{Cu} = 10$ eV, $U_O = 6$ eV, $V = \epsilon = t = 1$ eV. The energies of the one- and two-photon states, and that of the lowest singlet spin excitation m of the finite ring, relative to the ground state G are shown as an inset. Notice the near degeneracy of the one- and two-photon states. The transition dipole coupling μ_{21} is an order of magnitude larger than the coupling μ_{G1} .

FIG. 4. The transmission change induced by two temporally separated equivalent pump pulses. The pump and probe photon energies are 0.88 eV ($1.4 \mu\text{m}$) and 1.03 eV ($1.2 \mu\text{m}$), respectively. The relaxation time of the tail part is 1.2 ps. The transmission change with the second pump pulse is the same as that with the first. The accumulation of the tail part is observed by comparing with single-pulse response(not shown).

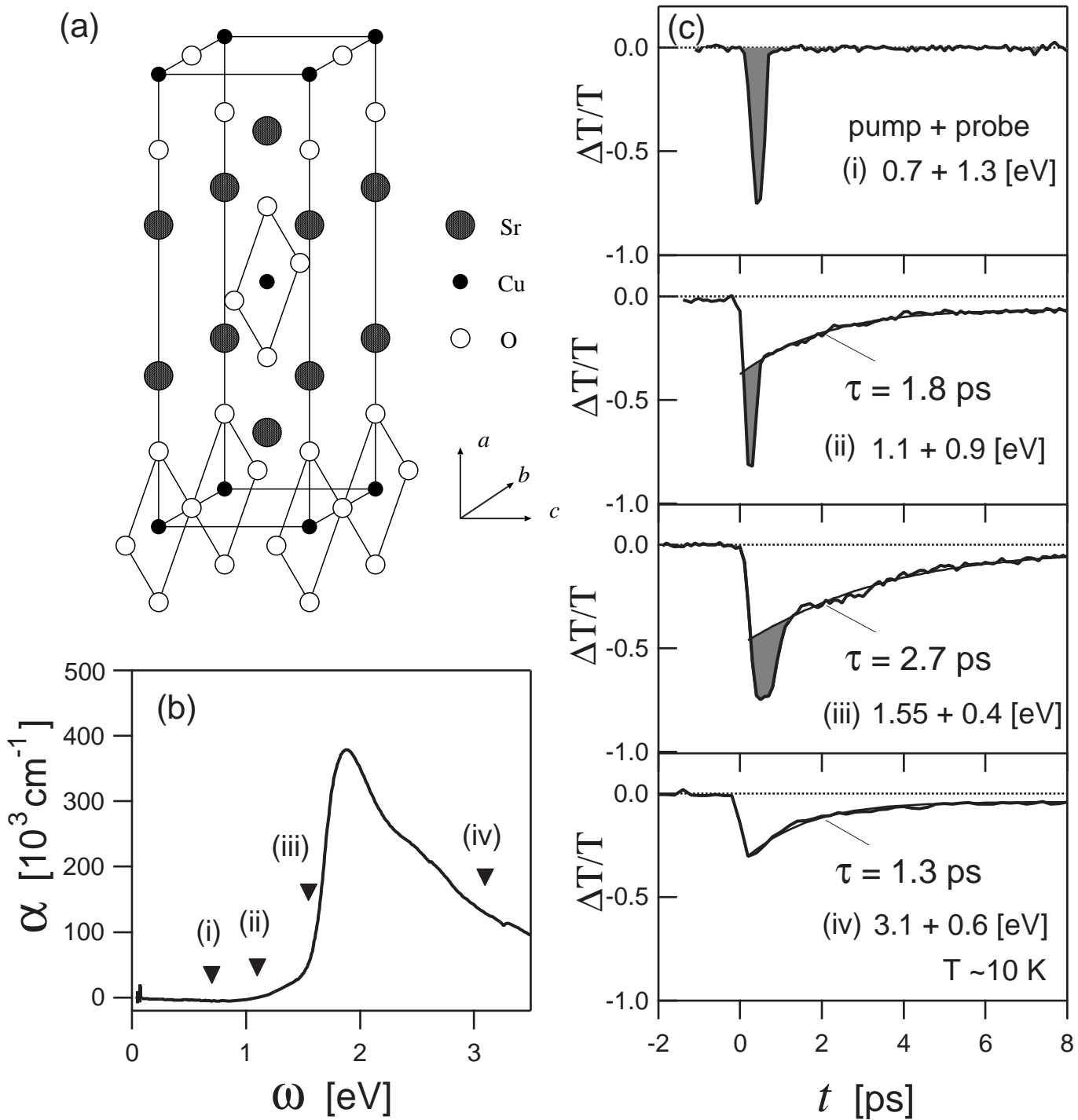


Fig.1 Ogasawara et al.

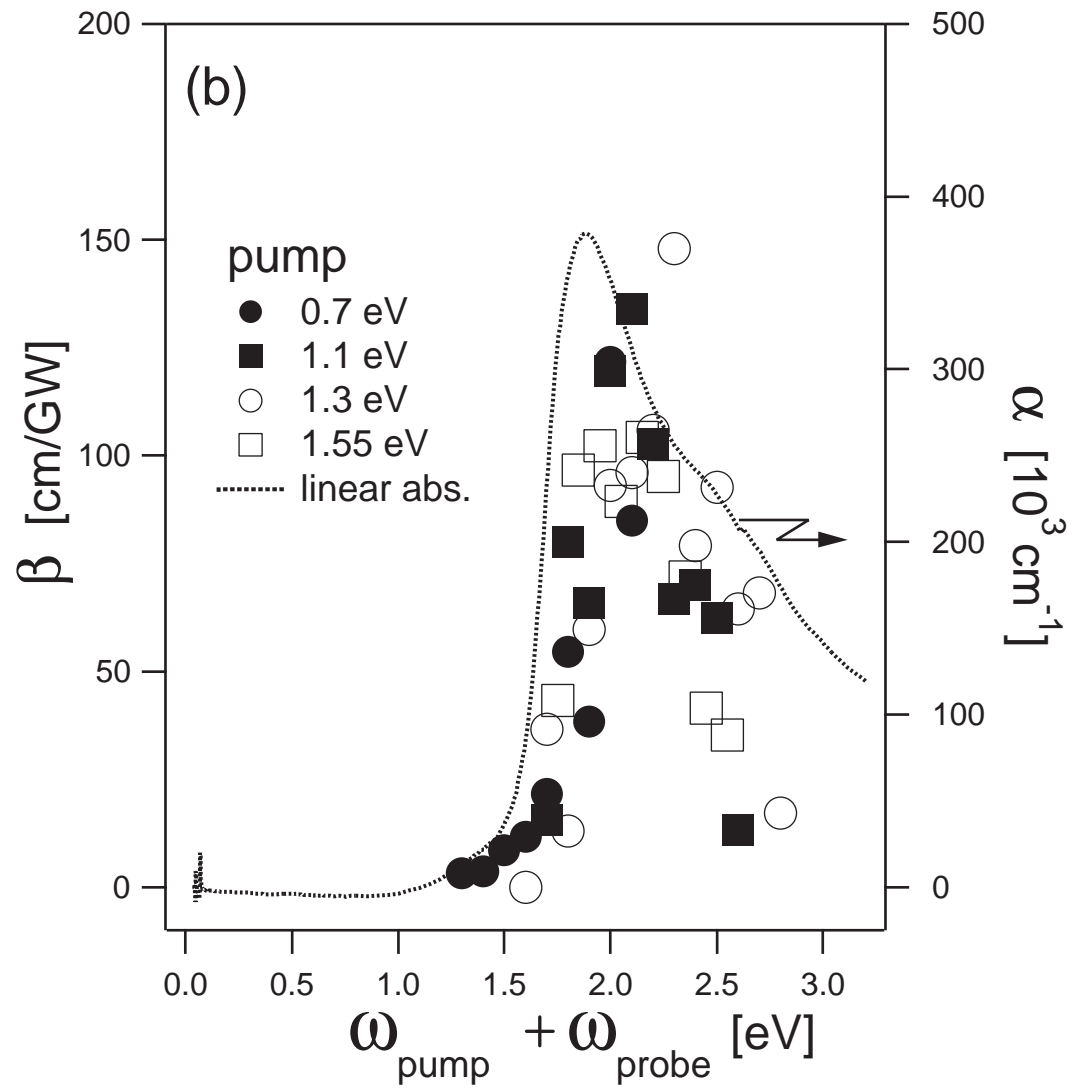
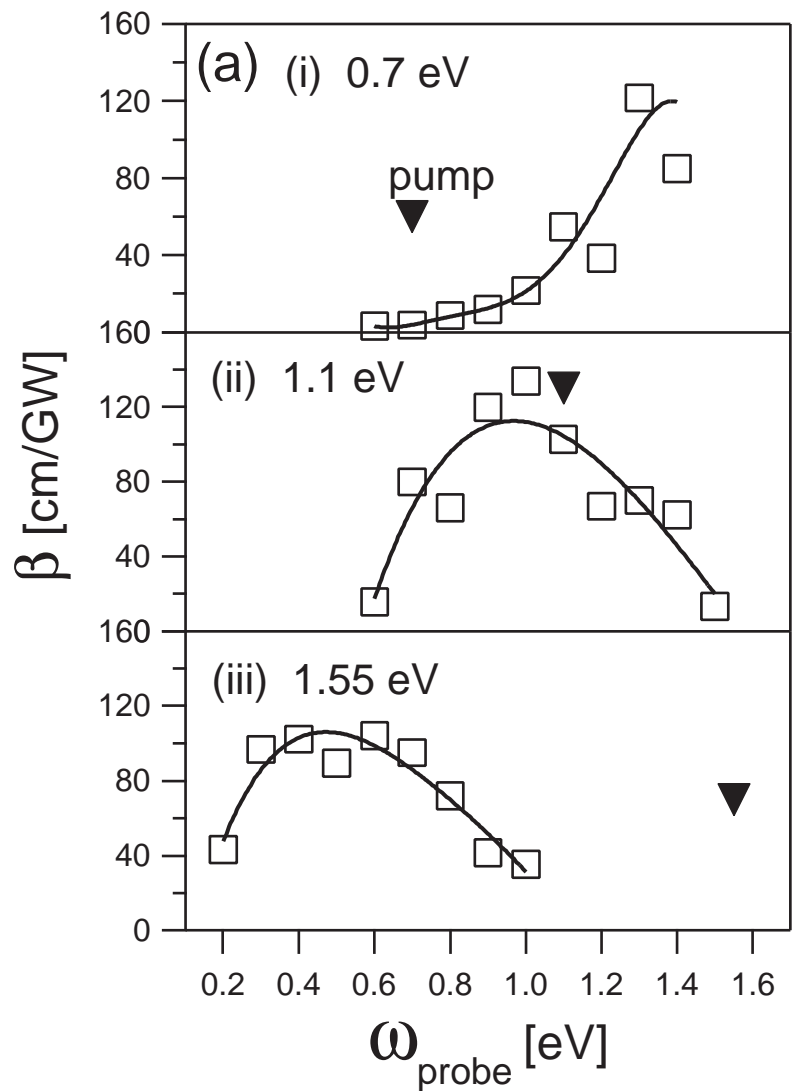
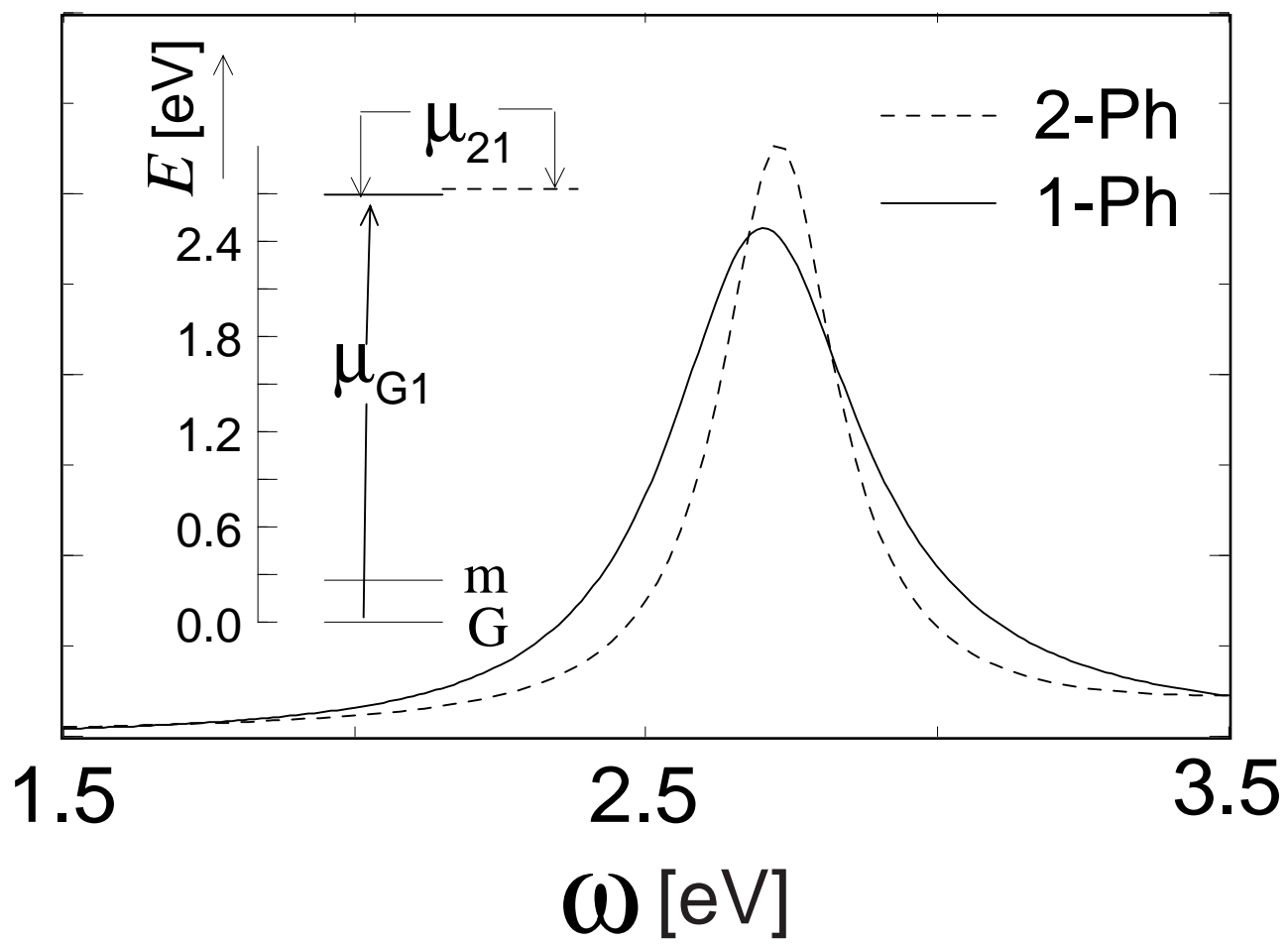


Fig.2 Ogasawara et al.



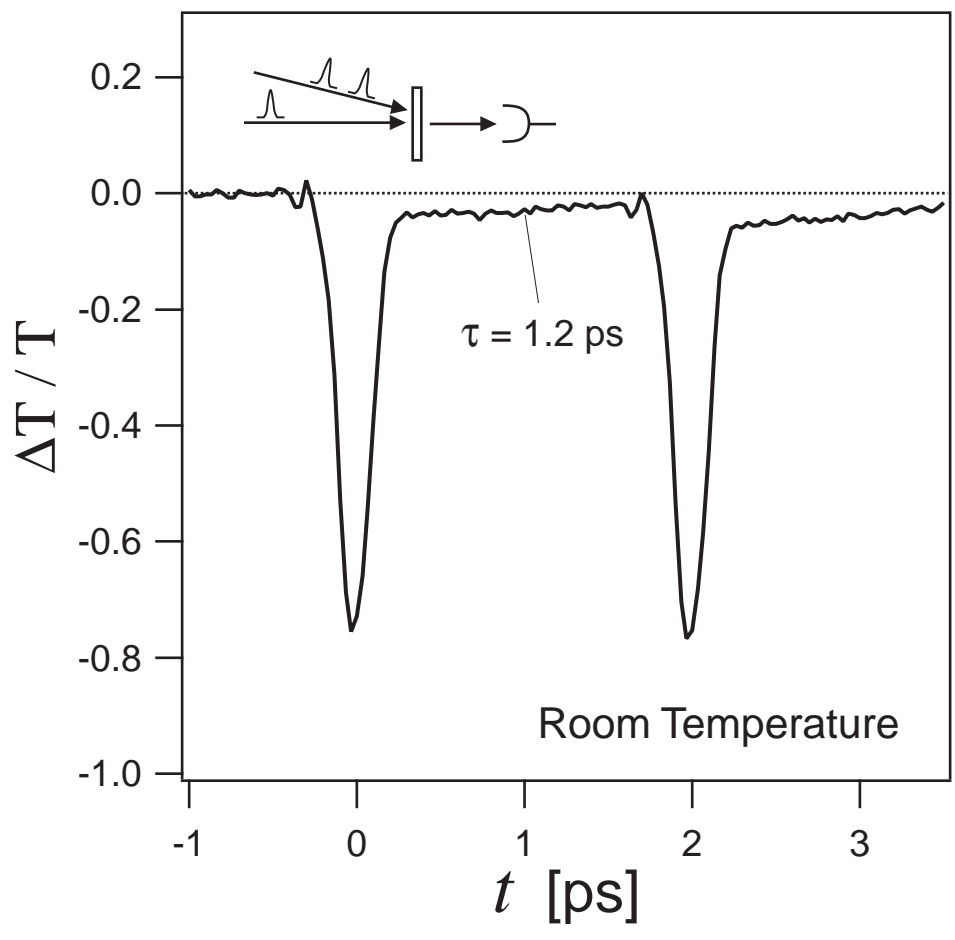


Fig. 4 Ogasawara et al.